

Published in final edited form as:

Lung Cancer. 2011 March ; 71(3): 271–282. doi:10.1016/j.lungcan.2010.06.002.

Anticancer activity of Noscapine, an opioid alkaloid in combination with Cisplatin in human non-small cell lung cancer

Mahavir Chougule, Apurva R. Patel, Pratik Sachdeva, Tanise Jackson, and Mandip Singh*
College of Pharmacy and Pharmaceutical Sciences, Florida A and M University, Tallahassee, FL 32307, USA

Abstract

The purpose of this study was to examine the efficacy of Noscapine (Nos) and Cisplatin (Cis) combination treatment in vitro in A549 and H460 lung cancer cells, in vivo in murine xenograft model and to investigate the underlying mechanism. The combination index values (<0.6) suggested synergistic effects of Nos + Cis and resulted in the highest increase in percentage of apoptotic NSCLC cells and increased expression of p53, p21, caspase 3, cleaved caspase 3, cleaved PARP, Bax, and decreased expression of Bcl₂ and surviving proteins compared with treatment with either agent. Nos + Cis treatment reduced tumor volume by 78.1 ± 7.5% compared with 38.2 ± 6.8% by Cis or 35.4 ± 6.9% by Nos alone in murine xenograft lung cancer model. Nos + Cis treatment decreased expression of pAkt, Akt, cyclin D1, survivin, PARP, Bcl₂, and increased expression of p53, p21, Bax, cleaved PARP, caspase 3, cleaved caspase 3, cleaved caspase 8, caspase 8, cleaved caspase 9 and caspase 9 compared to single-agent treated and control groups. Our results suggest that Nos enhanced the anticancer activity of Cis in an additive to synergistic manner by activating multiple signaling pathways including apoptosis. These findings suggest potential benefit for use of Nos and Cis combination in treatment of lung cancer.

Keywords

Lung cancer; Noscapine; Cisplatin; Combination chemotherapy; Apoptosis

1. Introduction

Lung cancer is one of the leading causes of cancer death and it is estimated that in the United States there will be 159,390 deaths in 2009 resulting from lung cancer accounting for 29% of all cancer deaths [1]. More than 85% of patients with lung cancer have non-small cell lung cancer (NSCLC). Chemotherapy with gemcitabine, taxanes or vinorelbine, together with a platinum drug is the first choice treatment in NSCLC [2,3]. Chemotherapy with Cisplatin (Cis) is associated with adverse side effects, such as anemia, neurotoxicity and nephrotoxicity [4]. Despite recent advances in chemotherapy, response rates in NSCLC remain <50% and a third of patients with stage IV disease have a 2-year survival rate of <20% [3,4]. To address this problem, attention has been focused on finding novel combination of anticancer agents with non-overlapping mechanisms of action to achieve enhanced efficacy with decreased side effects.

*Corresponding author at: College of Pharmacy and Pharmaceutical Sciences, Florida A and M University, 1520 M.Luther king Blvd, Tallahassee, FL 32307, USA. Tel.: +1 850 561 2790; fax: +1 850 599 3813. mandip.sachdeva@gmail.com (M. Singh).

Conflict of interest

None declared.

The effectiveness of microtubule-interfering agents in cancer therapy has been validated by the use of taxanes and vinca alkaloids for the treatment of variety of cancers [5]. However, the clinical success of taxanes + Cis combination treatment has been limited due to drug-resistance, need of i.v. infusion over a long period of time and associated severe toxicities [6,7]. Among antimicrotubule agents, the orally acting noscapinoids constitute an emerging class of compounds receiving considerable attention for treating cancers due to improved patient compliance and minimal side effects compared to taxanes [8–11]. Currently, phase I clinical trial of Noscapine (Nos) has been initiated for the treatment of relapsed or refractory multiple myeloma. Nos attenuates microtubule dynamics just enough to activate the mitotic checkpoints to stop cell cycle and do not alter the steady state monomer/polymer ratio of tubulin [12]. Nos was found to inhibit cell proliferation in wide variety of cancers [12–17] including many drug-resistant variants while evading normal [12–15]. Furthermore, Nos also showed little or no systemic toxicity to the body organs and did not inhibit primary humoral immune responses in mice [12,14,17]. Our previous studies demonstrated that oral administration of Nos showed significant reduction in tumor volume in NSCLC tumor xenograft in nude mice in a dose-dependent manner [18]. Landen et al. demonstrated that non-synergistic anticancer activity with Nos–Paclitaxel combination in murine B16LS9 melanoma model [12]. The use of Nos in combination with vincristine exhibits synergistic antitumor effects in leukemia cells in vitro [19]. However, anticancer potential of Nos in combination with approved anticancer agent in the treatment of lung cancer has not been explored yet. Nos in combination with anticancer agents may offer the possibility of effective management of cancer and thereby reduce dose and associated side effects. Therefore, there is a need for investigating the effect of Nos in combination with anticancer agents to realize its full chemotherapeutic potential in treatment of cancer.

The establishment of an optimal combination regimen with newer agents is an important step to improve the clinical outcome [20,21]. Several researchers have studied the combination of Cis and other agents and reported enhanced anticancer effects in treatment of lung cancer [22–28]. Both Nos and Cis have different mechanisms which may lead to potential additive/synergistic antitumor activity against lung cancer.

Therefore, we hypothesize that combination treatment of Nos with Cis may produce additive/synergistic antitumor activity in human NSCLC in vitro and in vivo possibly by enhancing multiple signaling pathway. This is the first report on the activity of the Nos in combination with Cis against lung cancer. The objectives of this study were to (a) examine the in vitro cytotoxicity and induction of apoptosis by Nos + Cis treatment against H460 and A549 cells and compare it to the Nos or Cis alone treatments and (b) evaluate the in vivo antitumor effect of Nos + Cis in murine H460 xenograft tumor model and investigate underlying mechanism.

2. Materials and methods

2.1. Materials

Noscapine and Cisplatin were purchased from Sigma Chemicals, St. Louis, MO, USA and Spectrum Chemicals, USA respectively. The human NSCLC cell lines H460 and A549 were obtained from American Type Culture Collection (Rockville, MD, USA). ApoTag Red *In Situ* Apoptosis detection kit[®] was purchased from Chemicon[®] International, CA, USA. DeadEnd[™] Colorimetric Apoptosis Detection System was purchased from Promega (Madison, WI). Antibodies against p53, p21, pAkt, cyclin D1, survivin, PARP, cleaved PARP, Bcl₂, Bax, caspase 3, cleaved caspase 3, caspase 8 and caspase 9, were purchased from Cell Signaling Technology (Beverly, MA). Antibody to β -actin and secondary HRP were purchased from Santa Cruz Biotechnology. The cleaved caspase 3 (175)

immunohistochemistry (IHC) kit was purchased from Cell Signaling (Beverly, MA). All other chemicals were either reagent or tissue culture grade.

2.2. Cell lines

H460 cells were grown in RPMI 1640 medium (Sigma, St. Louis, MO, USA) supplemented with 10% fetal bovine serum (FBS). A549 cells were grown in F12K medium (Sigma, St. Louis, MO, USA) supplemented with 10% FBS. All tissue culture media contained antibiotic antimycotic solution of penicillin (5000 U/ml), streptomycin (0.1 mg/ml), and neomycin (0.2 mg/ml). The cells were maintained at 37 °C in the presence of 5% CO₂ in air.

2.3. Animals

Female Nu/Nu mice (6 weeks old from Harlan, Indianapolis, IN) were grouped and housed ($n = 8$ per cage) in sterile microisolator caging unit supplied with autoclaved Tek-Fresh bedding. The animals were kept under controlled conditions of 12:12 h light:dark cycle, 22 ± 2 °C and 50 ± 15% relative humidity. The mice were fed (irradiated rodent chow Harlan Teklad) and autoclaved water ad libitum. The animals were housed at Florida A and M University in accordance with the standards of *the Guide for the Care and Use of Laboratory Animals* and the Association for Assessment and Accreditation of Laboratory Animal Care.

2.4. In vitro cytotoxicity studies

The cancer cell lines (A549 and H460) were plated in 96-well microtiter plates, at a density of 1×10^4 cells/well and allowed to incubate overnight. The cells were treated with various dilutions of Cis in the presence or absence of Nos at 10–30 and 30–50 μM against H460 and A549 cells respectively. The plates were incubated for 72 h at 37 ± 0.2 °C in a 5% CO₂-jacketed incubator. Cell viability in each treatment group was determined by crystal violet dye assay.

2.5. Data analysis for the combination treatments

The interactions between Cis and Nos were evaluated by the isobolographic analysis, a dose-oriented geometric method of assessing drug interactions [29,30]. For 50% toxicity, the combination index (CI) values were calculated based on the equation stated below:

$$CI = \frac{(D)_1}{(Dx)_1} + \frac{(D)_2}{(Dx)_2} + \alpha \frac{(D)_1(D)_2}{(Dx)_1(Dx)_2} \dots$$

where $(Dx)_1$: dose of drug 1 to produce 50% cell kill alone; $(D)_1$: dose of drug 1 to produce 50% cell kill in combination with $(D)_2$; $(Dx)_2$: dose of drug 2 to produce 50% cell kill alone; $(D)_2$: dose of drug 2 to produce 50% cell kill in combination with $(D)_1$; $\alpha = 0$ for mutually exclusive or 1 for mutually non-exclusive modes of drug action. CI > 1.3 antagonism; CI 1.1–1.3 moderate antagonism; CI 0.9–1.1 additive effect; CI 0.8–0.9 slight synergism; CI 0.6–0.8 moderate synergism; CI 0.4–0.6 synergism; CI 0.2–0.4 strong synergism.

2.6. Induction of apoptosis in H460 and A549 cells

To detect apoptotic cells, the ApoTag Red *In Situ* Apoptosis detection kit[®] (Chemicon[®] International, CA, USA) was used. Cells were plated at a density of 1×10^6 cells/well in 6-well plates and incubated overnight. H460 cells were treated with Cis (0.8 μM), or Nos (30 μM), or combination and A549 cells were treated with Cis (2.5 μM), or Nos (40 μM), or combination. Untreated cells were used as control. After 72 h, cells were fixed in 4% paraformaldehyde and mounted onto slides using Cytospin[®] (Shandon). Equilibration buffer

was added to slides and incubated for 10 min followed by incubation in working strength TdT enzyme at 37 °C for 1 h. The slides were incubated in stop/wash buffer for 10 min at room temperature. Working strength anti-digoxinenin conjugate (rhodamine) was added to each slide for 30-min incubation at room temperature. The images on the slides were visualized with an Olympus BX40 fluorescent microscope equipped with a computer-controlled digital camera (DP71, Olympus Center Valley, PA, USA). To quantify the apoptotic cells from terminal deoxynucleotidyl transferase-mediated nick end labeling (TUNEL) assay, 100 cells from 6 random microscopic fields were counted.

2.7. Western blot of NSCLC cells

Protein was extracted from untreated, Nos, Cis and Nos + Cis treated (72 h) cells in RIPA buffer (50 mM Tris-HCl, pH 8.0, with 150 mM sodium chloride, 1.0% Igepal CA-630 (NP-40), 0.5% sodium deoxychlorate, and 0.1% sodium dodecyl sulfate) with protease inhibitor (500 mM phenylmethylsulfonyl fluoride). Protein content was measured using BCA Protein Assay Reagent Kit (PIERCE, Rockford, IL). Equal amounts of supernatant protein (50 µg) from the control and different treatments were denatured by boiling for 5 min in SDS sample buffer, separated by 10% SDS-PAGE, transferred to nitrocellulose membranes for immunoblotting. Membranes were blocked with 5% skim milk in Tris-buffered saline with Tween 20 [10 mM Tris-HCl (pH 7.6), 150 mM NaCl, and 0.5% Tween 20] and probed with antibodies against p53 (1:500), p21 (1:500), caspase 3 (1:500), PARP (1:1000), cleaved PARP (1:1000), Bax (1:500), Bcl₂ (1:500), survivin (1:1000) and β-actin anti-bodies (Santa Cruz Biotechnology, Santa Cruz, CA). Horseradish peroxidase-conjugated secondary antibodies (Santa Cruz Biotechnology) were used. Enhanced chemiluminescent solution (Pierce) was used for detection.

2.8. In vivo antitumor effect of Nos against H460 lung tumors

The adherent H460 tumor cells were washed with PBS, harvested from confluent cultures by 5-min exposure to 0.25% trypsin and 0.02% EDTA solution in an incubator. Trypsinization was stopped with medium containing 10% FBS. The cell suspension was centrifuged at 500 × *g* for 4 min at 4 °C and the floating cells in the supernatant were discarded. The cell pellet was resuspended in medium containing 10% FBS and mixed thoroughly. Trypan blue staining was used to determine the number of viable cells. The resuspended cells were diluted to 3 × 10⁶ cells/100 µl in RPMI medium. The 100 µl of H460 cell suspension was injected subcutaneously into right flank area of each mouse [18]. The protocol for in vivo experiments with nude mice was approved by the Animal Care and Use Committee, Florida A and M University, Tallahassee, FL. The mice were randomized into vehicle control and treatment groups of eight animals each when xenografts were palpable with a tumor size in the range of 50 ± 15 mm³ on day 7 after tumor implantation. The control group received 160 µl of vehicle; the second group (*n* = 8) received Cis (2.5 mg/kg i.v. bolus, q4d × 3 schedule); the third group (*n* = 8) was given Nos 300 mg/kg daily by oral gavage; the fourth group (*n* = 8) received a combination of Cis and Nos. The sub-therapeutic dose of Cis (2.5 mg/kg i.v. bolus, q4d × 3 schedule) and Nos 300 mg/kg daily by oral gavage were selected based on our previous laboratory studies [18]. Treatment was started 7 days after tumor implantation and continued up to 38 days after tumor implantation. To check for evidence of toxicity, the animals were weighed weekly. The tumor dimensions were measured using a linear caliper and tumor volume was calculated using the equation $V (\text{mm}^3) = a \times b^2/2$, where *a* is the largest diameter and *b* is the smallest diameter. The mice were fed with food and water ad libitum. On day 38, all animals were sacrificed by exposure to a lethal dose of halothane in a desiccator. After dissection and removal of the tumor tissues, the tumors were washed in sterile PBS. For IHC and TUNEL assay procedures, some of the tumors were fixed in formalin while others were rapidly frozen in liquid nitrogen and stored at -80 °C.

2.9. Western blotting of tumor tissues

Tumor tissues harvested at 38 days after tumor implantation from control, Nos, Cis and combination treated mice were cut into small pieces and homogenized in PBS. The proteins were extracted using RIPA buffer [50 mM Tris-HCl, pH 8.0, with 150 mM sodium chloride, 1.0% Igepal CA-630, 0.5% sodium deoxycholate, and 0.1% sodium dodecyl sulfate (SDS)] with protease inhibitor (500 mM phenylmethylsulfonyl fluoride). Protein content was measured using BCA Protein Assay Reagent Kit (PIERCE, Rockford, IL). For WB, equal amounts of supernatant protein (50 µg) from the control and different treatments were denatured by boiling for 5 min in SDS sample buffer (0.25 M Tris-HCl pH 6.8, 8% SDS, 30% glycerol, 0.02% bromophenol blue and 10% 2-beta-mercaptoethanol), separated by 15% SDS-PAGE and transferred to nitrocellulose membranes for immunoblotting. The membranes were blocked with 5% skim milk in Tris-buffered saline with Tween 20 (10 mM Tris-HCl (pH 7.6), 150 mM NaCl, 0.5% Tween 20) and probed with p53 (1:500), p21 (1:500), pAkt (1:500), cyclin D1 (1:500), survivin (1:1000) PARP (1:1000), cleaved PARP (1:1000), Bax (1:500), Bcl₂ (1:500), cleaved caspase 3 (1:500), caspase 8 (1:500) and caspase 9 (1:500) and β-actin antibodies (1:500). Bound antibodies were revealed with HRP conjugated secondary antibodies (1:2000) using SuperSignal West pico chemiluminescent solution (PIERCE, Rockford, IL) upon exposure of X-ray film. β-Actin protein was used as a loading control. The expressions of proteins were normalized to loading controls (β-actin). Protein bands were subjected to densitometric analysis using open-source ImageJ software (v1.33u, NIH, USA). The expression values were expressed as percent ratio of protein expression to β-actin and control values were set to 100%.

2.10. TUNEL assay of xenograft lung tumor tissues

Formalin-fixed tumor tissues harvested 38 days after tumor implantation were embedded in paraffin and sectioned. DeadEnd™ Colorimetric Apoptosis Detection System (Promega, Madison, WI) was used to detect apoptosis in the tumor sections placed on slides according to the manufacturer's protocol. Briefly, the equilibration buffer was added to slides and incubated for 10 min followed by 10-min incubation in 20 µg/ml proteinase K solution. The sections were washed in PBS and incubated with TdT enzyme at 37 °C for 1 h in a humidified chamber for incorporation of biotinylated nucleotides at the 3'-OH ends of DNA. The slides were incubated in horseradish peroxidase-labeled streptavidin to bind the biotinylated nucleotides followed by detection with stable chromagen DAB. The images on the slides were visualized with an Olympus BX40 light microscope equipped with a computer-controlled digital camera (DP71, Olympus Center Valley, PA, USA). Three slides per group were stained and apoptotic cells were identified by dark brown cytoplasmic staining.

2.11. Immunohistochemistry for cleaved caspase 3 expression

Sections prepared from formalin-fixed, paraffin-embedded lung tissues were used for IHC studies according to the protocol specified in the SignalStain™ Cleaved Caspase-3 (Asp 175) IHC kit (Cell Signaling, Beverly, MA). The section slides were washed in xylene and hydrated in different concentrations of alcohol. The slides were heated in 0.1 M sodium acetate solution at 95 °C for 10 min for antigen retrieval. The slides were washed three times in PBS and incubated with the primary antibody against cleaved caspase 3 overnight at 4 °C. Horseradish peroxidase-conjugated secondary antibody was applied to locate the primary antibody. The specimens were stained with Nova Red stain and counterstained with hematoxylin. The presence of brown staining was considered a positive identification for activated caspase 3. The Olympus BX40 light microscope equipped with computer-controlled digital camera (DP71, Olympus Center Valley, PA, USA) was used to visualize the images on the slides.

2.12. Statistics

One-way ANOVA followed by Tukey's Multiple Comparison Test was performed to determine the statistical significance of differences among groups using GraphPad PRISM version 3.0 software (SanDiego, CA). Differences were considered statistically significant in all experiments at $P < 0.01$ (*significantly different from untreated controls; **significantly different from Nos and Cis single treatments, (■) significantly different from Cis single treatment unless otherwise stated).

3. Results

3.1. In vitro cytotoxicity of Cis and Nos combination

Nos inhibited proliferation of H460 and A549 cells in a dose-dependent manner with IC_{50} values of $34.7 \pm 2.5 \mu\text{M}$ and $61.25 \pm 5.6 \mu\text{M}$ respectively. Cis showed IC_{50} of $1.4 \pm 0.1 \mu\text{M}$ and 4.2 ± 0.2 against H460 and A549 NSCLC cells. The IC_{50} values of Nos against NSCLC cells are comparable to the cytotoxic effects observed with murine melanoma [12] B16LS9 cells ($IC_{50} = 50 \mu\text{M}$), human ovarian [13] 1A9PTX10 cells ($IC_{50} = 22.7 \mu\text{M}$), HeLa ($IC_{50} = 25 \mu\text{M}$) and thymocyte ($IC_{50} = 10 \mu\text{M}$) cells [17]. The combined effects of Cis and Nos on cell proliferation were evaluated by isobolographic analysis method. The CI values ranged from 0.31 ± 0.5 to 0.57 ± 0.4 for 50% cell kill suggesting synergistic to strong synergistic behavior between Nos concentration in the range of 10–50 μM and Cis against both NSCLC cell lines (Table 1).

3.2. Induction of apoptotic DNA fragmentation in H460 and A549 cells

TUNEL assay was used to identify 3'-hydroxyl end of fragmented DNA, which is one of the biochemical markers of apoptosis. Fig. 1A and B shows that apoptosis is induced in H460 and A549 cells following treatment with Cis, or Nos, or their combination. Nos + Cis treatment led to apoptosis in $67 \pm 5\%$ of treated H460 cells compared to $25 \pm 4\%$ and $21 \pm 3\%$ in Cis and Nos respectively after 72 h (Fig. 1C). Similarly, combination treatment against A549 cells led to $62 \pm 6\%$ apoptosis compared to $22 \pm 6\%$ and $19 \pm 5\%$ in Cis and Nos respectively (Fig. 1D). All treatments were significantly different from control ($*P < 0.01$). Cis or Nos treatment was significantly different from treatment with the combination of Cis and Nos ($**P < 0.01$).

3.3. Effects of treatments on apoptotic proteins in H460 and A549 NSCLC cells

To further study the role of apoptosis induced by Nos and Cis, we evaluated expression of p53, p21, caspase 3, cleaved caspase 3, PARP, cleaved PARP, Bax, Bcl₂, survivin proteins by western blotting performed on whole-cell lysates from control and treated H460 and A549 cells and results were graphically presented in Fig. 2A–C. Combination treatment significantly ($*, **P < 0.01$) increased p53 and p21 proteins levels by ~2.1- and ~1.9-fold compared to control respectively. The combination, Nos and Cis decreased expression of PARP to ~0.50-, ~0.12-, and ~0.20-fold and increased expression of cleaved PARP to ~2.2-, ~1.13-, and ~1.18-fold respectively as compared to controls. Combination increased caspase 3 and cleaved caspase 3 expression to ~1.9- ($*, **P < 0.01$) and ~2.1-fold after treatment for 72 h respectively. Nos + Cis significantly ($*, **P < 0.01$) decreased Bcl₂ expression and increased Bax expression ($*, **P < 0.01$) compared to controls after treatment for 72 h. The combination decreased survivin expression by ~0.68-fold ($*, **P < 0.01$) compared to a ~0.35-fold ($*P < 0.05$) increase by Cis or ~0.28-fold ($*P < 0.05$) Nos alone.

3.4. Antitumor effect of Cis + Nos in a s.c. xenograft model

The in vivo anticancer activity of Nos in combination with Cis was further investigated in female athymic nude mice bearing H460 xenograft lung tumors. The results (Fig. 3A and B)

show that tumor volume significantly decreased after treatment with Cis (2.5 mg/kg i.v., * $P < 0.01$), Nos (300 mg/kg oral, * $P < 0.01$), or Cis + Nos (*, ** $P < 0.01$) compared to control. It is evident that Cis + Nos was most effective in inhibiting tumor growth compared to Cis or Nos treatments. At the end of the study period (31 days of treatment period, i.e. 38 days after tumor implantation), there was $78.1 \pm 7.5\%$ reduction in tumor volume by the combination treatment of Cis + Nos compared to $38.2 \pm 6.8\%$ by Cis, or $35.4 \pm 6.9\%$ by Nos alone. Furthermore, we did not observe any weight loss or other signs of toxicity in the mice treated with combination and single-agent treatment (Fig. 3C).

3.5. Effects of treatments on apoptotic proteins in H460 xenograft lung tumors

We compared expression of several apoptotic proteins in tumor lysates from control and treated mice by western blot analysis using β -actin as loading control (Figs. 4 and 5). Nos, Cis and Nos + Cis treatment significantly (* $P < 0.01$) increased expression of p53 to 1.84-, 1.41- and 1.35-fold in regressed tumor samples compared to control respectively. Nos + Cis treatment showed significant (*, ** $P < 0.01$) increase in expression of p53 compared to Nos or Cis treatment (Fig. 4A and B). Expression of p21 was significantly (*, ** $P < 0.01$) increased to 1.24-fold with Nos + Cis treatment compared to 1.15- and 1.14-fold with Nos and Cis treatment respectively (Fig. 4A and B). In regressed tumors, Nos + Cis, Nos and Cis treatment showed significant (*, ** $P < 0.01$) decrease in expression of Akt, pAkt and cyclin D1 compared to control group (Fig. 4A and B). Expression of cell survival protein survivin was decreased significant ($P < 0.01$) to 0.68-, 0.32- and 0.29-fold following Nos + Cis, Cis and Nos treatment compared to control tumors respectively (Fig. 4A and B). Furthermore, Nos + Cis treatment showed significant (* $P < 0.01$) increase in expression of Bax and decrease in expression of Bcl₂ compared to single-agent treated and control groups. Nos + Cis, Cis, and Nos treatment decreased expression of Bcl₂ to 0.38-, 0.16- and 0.19-fold in harvested tumors compared to control tumors (Fig. 5A and B). Results illustrated in Fig. 4A and B show that Nos + Cis treatment showed significant (*, ** $P < 0.01$) increase in expression of cleaved PARP, caspase 8, cleaved caspase 8, caspase 9, cleaved caspase 9, caspase 3, and cleaved caspase 3 and decrease in expression of PARP compared to control treatment groups (Fig. 5A and B). The expression of apoptotic and antiapoptotic proteins (cleaved PARP, caspase 8, caspase 3, cleaved caspase 3 and PARP) in Nos + Cis treatment was significantly (** $P < 0.01$) different from single-agent treatment groups. In Nos + Cis treated tumors the expression of caspase 9 was significantly (*, ■, $P < 0.01$) different from Cis treated and control groups (Fig. 5A and B).

3.6. Effects of Cis and Nos on DNA fragmentation in H460 xenograft lung tumors

To further investigate the role of apoptosis, harvested tumor sections were stained with TUNEL for detection of DNA fragmentation (Fig. 6A and C). Single-agent therapy with either Nos or Cis induced DNA fragmentation (brown staining) that was further increased by Nos + Cis treatment. Nos + Cis treatment led to apoptosis in $61 \pm 8\%$ of the tumor cells, whereas Nos and Cis induced apoptosis in $32 \pm 5\%$ and $30 \pm 6\%$ of the tumor cells respectively. All treatments were significantly different from control (* $P < 0.01$). Nos + Cis treatment showed significant (*, ** $P < 0.01$) increase in induction of apoptosis in regressed tumors compared to single-agent treatment (Fig. 6A and C).

3.7. Cleaved caspase 3 expression in H460 xenograft lung tumors

Expression of cleaved caspase 3 was also investigated in the control and treated tumors by IHC analysis. Cis, Nos, and Cis + Nos treatment induced caspase 3 expression in tumors compared to control tumors. Combination, Cis and Nos treatment showed $55 \pm 3.6\%$, $33 \pm 2.1\%$, and $25 \pm 2.0\%$ increased expression of caspase 3 in tumors tissues respectively compared to control group (Fig. 6B and D).

4. Discussion

Poor clinical outcome of the current chemotherapy avenues has prompted the need for new therapeutic strategies for treatment of lung cancer. Platinum based combination chemotherapy is the standard therapy for NSCLC [2,3]. However, the efficacy and safety of this treatment are limited and the 5-year survival rate is only 15% [4]. Among anticancer agents, antimicrotubules constitute one of the promising chemotherapeutic agents for treatment of lung cancers [5]. Clinical use of currently available antimicrotubular agents has been limited due to drug-resistance, prolonged i.v. infusion and associated adverse side effects [6,7]. Nos is considered as safe orally active antimicrotubule agent that alters microtubule dynamics without affecting the microtubule polymer mass [12,14,17] and demonstrated promising in vitro and in vivo antitumor activity against variety of cancers including resistant type [12–17]. Our previous studies demonstrated that Nos has promising anticancer activity in a dose-dependent manner against NSCLC without exerting adverse side effects [18]. The anticancer activity that Nos has demonstrated in NSCLC in which the platinum analogues are among the most active agents has been the impetus for the development of Nos/platinum combination regimens. Therefore, we evaluated the potential of Nos in potentiating antitumor activity of Cis in in vitro and in vivo against NSCLC and elucidated mechanistic pathways that contribute to the antitumor responses. This is the first study that demonstrated additive to synergistic behavior of Nos and Cis combination treatment against lung cancer.

We have selected fast growing H460 and slow growing A549 cells [31] to ascertain interaction between Nos and Cis using isobolographic method [29,30] and TUNEL assay. Isobolographic analysis of the data showed that Nos at 10–30 μM and 30–50 μM concentration enhanced the cytotoxicity of Cis in H460 and A549 NSCLC cells in a synergistic to strongly synergistic manner respectively (Table 1). We have selected Nos concentration of 10 μM , 20 μM and 30 μM of Nos against H460 cells and 30 μM , 40 μM , 50 μM against A549 cells, which were lower than IC_{50} value to ascertain the interaction between Nos and Cis. We recently reported that the CI values < 1.0 are indicative of synergistic interactions between DIM-C-pPhC₆H₅ and Docetaxel [30]. Our results are consistent with the work of Bigioni et al. who demonstrated the cytotoxicity of Cis in H460 cells was synergistically modified by Sabarubicin [22]. Synergistic interactions were also reported for sulindac sulfide, exisulind, and nordihydroguaiaretic acid with paclitaxel, Cis, and 13-cis-retinoic acid against A549, H460, and SHP77 human lung cancer cell lines [23]. Hiser et al. demonstrated that Nos in combination with vincristine showed synergistic interaction with CI values of < 1 against acute lymphoblastic CCRF-CEM and acute myelogenous leukemia HL-60 cells. A combination of Nos with vincristine showed protection against demyelination in vitro and thereby may decrease the neurotoxicity associated with vincristine [19]. However, the in vivo efficacy of Nos and vincristine combination has not been evaluated.

To study the mechanism involved in the enhanced cytotoxicity of Cis by Nos, we evaluated the induction of apoptosis in H460 and A549 cells after treatment for 72 h. The TUNEL assay results showed statistically significant (*, ** $P < 0.01$) induction of apoptosis in combination treatment compared to single agent (Fig. 1A–D) which suggest the synergistic interaction between Cis and Nos. Similar to our results, combination treatment of Cis and liposomal honokiol showed significant (*, ** $P < 0.01$) positive TUNEL staining in A459 regressed tumor tissues compared to single-agent treatment [24].

Since data from TUNEL assay provided evidence of enhanced apoptosis induction with Nos and Cis combination, we examined the effects of several proapoptotic responses using whole tissue lysate. Fig. 2 demonstrates that simultaneous co-treatment of Nos and Cis increased

expression of p53, p21, Bax and decreased expression of Bcl₂ at 72 h compared to single-agent treatment and control. Activation of p53 protein plays a crucial role in the control of tumor cell response to chemotherapeutic agents and DNA-damaging agents. p21 and Bax, downstream effectors of p53, were activated in combination treatment producing apoptosis in lung tumor cells. In support of our data, Aneja et al. showed that Nos activates growth arrest and apoptosis primarily via a p53-dependent pathway against colon cancer cells [32]. Furthermore, our western blot results showed a significant (*, ***P* < 0.01) increase in expression of cleaved PARP, caspase 3 and cleaved caspase 3 following combination treatment after 72 h compared to treatment with the compounds alone (Fig. 2A–C). These results suggest that apoptosis may be mediated through the mitochondrial pathway via down-regulation of antiapoptotic Bcl₂ and up-regulation of proapoptotic Bax. Proapoptotic (Bax and Bak) and antiapoptotic (Bcl-2 and Bcl-xL) members of the Bcl-2 family of proteins sensitize cells to and protect them from apoptosis respectively [33]. Proapoptotic proteins increase mitochondrial permeability unlike the antiapoptotic proteins, which block this process [33]. Therefore, we reasoned that cell damage resulting from treatment possibly caused Bax to bind to Bcl₂ allowing the release of cytochrome c from the mitochondria. Our findings related to the increase in Bax/Bcl₂ ratio indicated similar line of evidence of involvement of mitochondrial pathway in Nos induced apoptosis reported with human myelogenous leukemic and human colon cancer cells [15,32]. Interaction of cytochrome c with Apaf-1 (apoptotic protease activating factor-1) results in activation of caspase 9. Caspase 9 then activates caspase 3, which cleaves specific key substrates such as PARP leading to apoptotic cell death. In addition we also observed that Cis, Nos and Nos + Cis treatment decreased survivin in the lung cells (Fig. 2A–C). Survivin is a member of the inhibitor of apoptosis family which inhibits caspase activation and acts as a negative regulator [34]. Therefore, the down-regulation of survivin expression results in activation of caspases and thereby induces apoptosis in tumor cells. Similar to our results, treatment of human leukemia and myeloma cells with Nos (25 μm) showed decreased expression of survivin [35].

Having established the effectiveness of the combination treatment in vitro, we next evaluated the in vivo antitumor efficacy of Cis + Nos in faster growing H460 xenograft lung tumors in Nu/nu mice. The overall pattern of antitumorigenic activity is summarized in Fig. 3A which shows that Nos treatment with 300 mg/kg/day enhanced antitumorigenic activity of Cis (2.5 mg/kg i.v., q4d × 3 schedules). Tumor volume for the Nos + Cis treatment averaged 525.3 ± 56.9 mm³ compared with 1450.2 ± 404.8 mm³ for Nos alone or 1522.6 ± 310.1 mm³ for Cis alone (tumor volume ± SE) on day 38 post-tumor implantation. The Nos + Cis treatment showed a significant (*, ***P* < 0.01) decrease in tumor volume compared to controls or either agent (Fig. 3B). We selected sub-therapeutic dose of Nos, i.e. 300 mg/kg based on our previous studies which have demonstrated dose-dependent anti-cancer activity (300 < 450 < 550 mg/kg/day) of Nos against H460 xenograft murine model [18]. However, other researchers have assessed the antitumor activity of Nos against variety of tumors; e.g. melanoma tumors at 300 mg/kg/day oral [12], lymphoma tumors at 120 mg/kg/day, oral [14] and human breast tumors at 120 mg/kg/day, intraperitoneally [17]. Previous studies demonstrated that anticancer activity of Nos varies with the type and sensitivity of cancer cells [12]. Results in Fig. 3C showed non-significant (*P* > 0.01) change in weight loss in Nos, Cis, and Nos + Cis treatment groups suggest dosage levels used in this investigation were tolerable in mice [12,14,17]. Nos + Cis treatment will be advantageous over conventional taxane + Cis treatment in treatment of lung cancer due to improved patient compliance by oral administration of Nos and minimal adverse side effects. Landen et al. studied in vivo anticancer activity of Nos at 300 mg/kg alone and in combination with 25 mg/kg paclitaxel i.p. injected on days 4, 6, 10, 12, 14, and 16 against B16LS9 murine xenograft melanoma model. Nos anticancer activity (tumor volume 1311 ± 415 mm³) was comparable to that of paclitaxel (tumor volume 1597 ± 612 mm³) without exerting

observable side effects. However, the additive or synergistic effect between Nos–Paclitaxel (tumor volume, $1000 \pm 239 \text{ mm}^3$) was not observed and this combination was also not further investigated [12]. In present investigation, we have evaluated in vitro and in vivo antitumor activity of Nos–Cis combination including underlying mechanisms. Nos + Cis combination treatment showed synergistic interaction in vitro and additive to synergistic activity in xenograft model. The in vivo additive to synergistic activity of Nos + Cis combination treatment which may be attributed to: (a) poor bioavailability (<30%), (b) short plasma half life (<4.5 h) and (c) extensive first-pass metabolism of Nos that reduces its availability at the tumor site [36–38]. Our future studies will focus on improving the bioavailability of Nos to explore its anticancer potential in combination with anticancer agents.

Several studies have provided evidence that enhanced tumor growth inhibition can be achieved by combining Cis with other agents such as Sabarubicin [22], liposomal honokiol [24], SN-38 [25], lexatumumab [26], thalidomide [27], and All-trans-retinoic acid [28]. In vivo studies by Liu et al. showed that the All-trans-retinoic acid enhance the antitumor activity of Cis in vivo in melanoma-bearing mice [28] and these results are consistency with those observed in this study.

Previous studies demonstrated that Nos induces multiple proapoptotic responses that induce the apoptosis against variety of tumors [12–17]. Our results indicate that simultaneous co-treatment of Cis and Nos significantly (*, ** $P < 0.01$) increased expression of p53, p21 and Bax compared to single-agent treatment and control (Fig. 4A and B). Our results demonstrate that Cis and Nos alone and Nos + Cis treatment induced proapoptotic Bax or decreased survivin and Bcl₂ proteins and this was also accompanied by down-regulation of cyclin D1 (Fig. 4A and B). These results also suggest that apoptosis may be mediated through the mitochondrial pathway via down-regulation of anti-apoptotic Bcl₂ and up-regulation of proapoptotic Bax [33]. The cell damage resulting from treatment possibly caused Bax to bind to Bcl₂ allowing the release of cytochrome c followed by interaction with Apaf-1 which results in activation of caspase 9. Furthermore, the decreased expression of cyclin D1 suggests involvement of ubiquitin/proteasome system in induction of apoptosis by Nos + Cis. Ubiquitin/proteasome system regulates various cell cycle regulators and transcription factors such as p53, cyclins, and cyclin-dependent kinase inhibitors [39]. In addition we also observed that Cis, Nos and Nos + Cis treatment decreased cell survival proteins Akt, pAkt and survivin in the lung tumors (Fig. 3A and B). Our western blot results obtained with lung tumor tissues correlate well with expression of protein markers under in vitro conditions with H460 and A549 NSCLC cells (Fig. 2A–C).

The role of apoptosis in Nos + Cis treatment was further investigated by determining expression of various apoptotic proteins such as PARP, caspase 3, caspase 8, and caspase 9 in regressed tumors. Fig. 5A and B indicates that Cis + Nos treatment significantly (*, ** $P < 0.01$) increased expression of cleaved PARP, capases 3, cleaved capases 3, caspase 8, and caspase 9 compared to single-agent treatment and control. Our in vitro western blot results also showed increase in expression of caspase 3 and cleaved caspase 3 following Nos or Cis or Nos + Cis treatment against H460 and A549 cells (Fig. 2A–C). Caspases are critical protease mediators of apoptosis triggered by different stimuli [26,29]. In the present study, we found that the Nos + Cis treatment activated initiator caspases, such as caspase 8, cleaved caspase 8, caspase 9 cleaved caspase 9, and effector caspases caspase 3 (Fig. 5A and B). Consistent with our results Wu and Kakehi demonstrated synergistic cytotoxicity of lexatumumab and Cis against renal cell carcinoma cells by potentiation of the extrinsic and intrinsic apoptotic pathways [26].

Furthermore, to support the possible involvement of apoptosis in the antitumor effects of Nos + Cis, we studied induction of apoptosis by TUNEL assay and expression of cleaved caspase 3. DNA fragmentation was highly induced by Nos + Cis treatment compared to Nos or Cis alone thus confirming that apoptosis is an important pathway associated with the anticancer activity of these compounds (Fig. 6A and C). These in vivo responses correlated with induced DNA fragmentation observed in H460 and A549 cells treated with the same compounds (Fig. 1A–D). Increased expression of cleaved caspase 3 (Fig. 6B and D) was also observed in tumors treated with Nos + Cis compared to tumors treated with Cis or Nos alone. Our results showed that tumor regression induced by Nos + Cis treatment was also mediated through increased expression of effector caspase 3 and correlated very well with our caspase 3 expression results obtained with western blots of tumor tissue lysates (Fig. 5) and tumor cell lysates (Fig. 2). Our previous studies also demonstrated induction of apoptosis and activation of cleaved caspase 3 following Nos treatment in the dose range of 300–550 mg/kg/day [18]. In support of our results, Ye et al. demonstrated increased apoptotic activity in regressed MCF-7 breast cancer and Renal 1983 tumors following 120 mg/kg/day Nos treatment in mice [17]. Cis has been effective in inducing apoptosis against lung [24], melanoma [40], ovarian [41] and renal cell [26] cancers and this effect was correlated with DNA damage by forming DNA-Pt adducts and DNA strand breaks. Consistent with our data, liposomal honokiol + Cis treatment led to significant ($P < 0.05$) increases in percentage of apoptotic cells in A459 lung tumor xenografts compared to single-agent therapy [24]. Our findings suggest that the activation of extrinsic and intrinsic apoptotic pathways plays a critical role in the additive to synergistic cytotoxicity of Nos + Cis treatment against lung tumor cells. To gain more insights on the anticancer mechanisms of Nos and Cis, other non-apoptotic signaling pathways including angiogenesis need to be investigated and these studies are in progress.

In conclusion, results of this study demonstrated that combination of Nos and Cis is highly effective for inhibiting lung tumor growth in a murine xenograft model for lung cancer. The antitumorigenic activity of Cis was enhanced by Nos through induction of apoptosis via intrinsic and extrinsic pathways, activation of growth inhibitory, and inhibition of survival proteins in lung tumors. Thus the use of Nos and Cis combination therapy could be a novel approach for the treatment for lung cancer and possibly reduce the adverse side effects associated with platinum based chemotherapy.

Acknowledgments

The authors acknowledge the financial support provided by RCMI award (G12RR03020-11) and NIGMS/MBRS award (5S06GM008111-36) from NIH.

References

1. http://www.cancer.org/docroot/CRI/content/CRI_2_4_1x_What_Are_the_Key_Statistics_About_Lung_Cancer_15.asp?sitearea=.
2. Wakelee H, Belani CP. Optimizing first-Line treatment options for patients with advanced NSCLC. *Oncologist*. 2005; 10:1–10. [PubMed: 16368866]
3. Fleming S, Lucas F, Schofield MA. Therapeutic area review of oncology products and players. *Expert Opin Emerg Drugs*. 2001; 6:317–29. [PubMed: 15989529]
4. Douillard JY, Eckardt J, Scagliotti GV. Challenging the platinum combinations in the chemotherapy of NSCLC. *Lung Cancer*. 2002; 38:21–8. [PubMed: 12480191]
5. Jordan MA. Mechanism of action of antitumor drugs that interact with microtubules and tubulin. *Curr Med Chem Anticancer Agents*. 2002; 2:1–17. [PubMed: 12678749]
6. Van Zuylen L, Verweij J, Sparreboom A. Role of formulation vehicles in taxane pharmacology. *Invest New Drugs*. 2001; 19:125–41. [PubMed: 11392447]

7. Markman M. Managing taxane toxicities. *Support Care Cancer*. 2003; 11:144–7. [PubMed: 12618923]
8. Anderson JT, Ting AE, Boozer S, Brunden KR, Crumrine C, Danzig J, et al. Identification of novel and improved antimitotic agents derived from noscapine. *J Med Chem*. 2005; 48:7096–8. [PubMed: 16279766]
9. Anderson JT, Ting AE, Boozer S, Brunden KR, Danzig J, Dent T, et al. Discovery of S-phase arresting agents derived from noscapine. *J Med Chem*. 2005; 48:2756–8. [PubMed: 15828811]
10. Aneja R, Zhou J, Vangapandu SN, Zhou B, Chandra R, Joshi HC. Drug-resistant T-lymphoid tumors undergo apoptosis selectively in response to an antimicro-tubule agent, EM011. *Blood*. 2006; 107:2486–92. [PubMed: 16282340]
11. Zhou J, Gupta K, Aggarwal S, Aneja R, Chandra R, Panda D, et al. Brominated derivatives of noscapine are potent microtubule-interfering agents that perturb mitosis and inhibit cell proliferation. *Mol Pharmacol*. 2003; 63:799–807. [PubMed: 12644580]
12. Landen JW, Lang R, McMahon SJ, Rusan NM, Yvon AM, Adams AW, et al. Noscapine alters microtubule dynamics in living cells and inhibits the progression of melanoma. *Cancer Res*. 2002; 62:4109–14. [PubMed: 12124349]
13. Zhou J, Gupta K, Yao J, Ye K, Panda D, Giannakakou P, et al. Paclitaxel-resistant human ovarian cancer cells undergo c-Jun NH2-terminal kinase-mediated apoptosis in response to noscapine. *J Biol Chem*. 2002; 277:39777–85. [PubMed: 12183452]
14. Ke Y, Ye K, Grossniklaus HE, Archer DR, Joshi HC, Kapp JA. Noscapine inhibits tumor growth with little toxicity to normal tissues or inhibition of immune responses. *Cancer Immunol Immunother*. 2000; 49:217–25. [PubMed: 10941904]
15. Heidari N, Goliaei B, Moghaddam PR, Rahbar-Roshandel N, Mahmoudian M. Apoptotic pathway induced by noscapine in human myelogenous leukemic cells. *Anticancer Drugs*. 2007; 18:1139–47. [PubMed: 17893514]
16. Landen JW, Hau V, Wang M, Davis T, Ciliax B, Wainer BH, et al. Noscapine crosses the blood-brain barrier and inhibits glioblastoma growth. *Clin Cancer Res*. 2004; 10:5187–201. [PubMed: 15297423]
17. Ye K, Ke Y, Keshava N, Shanks J, Kapp JA, Tekmal RR, et al. Opium alkaloid noscapine is an antitumor agent that arrests metaphase and induces apoptosis in dividing cells. *Proc Natl Acad Sci USA*. 1998; 95:1601–6. [PubMed: 9465062]
18. Jackson T, Chougule MB, Ichite N, Patlolla RR, Singh M. Antitumor activity of noscapine in human non-small cell lung cancer xenograft model. *Cancer Chemother Pharmacol*. 2008; 63:117–26. [PubMed: 18338172]
19. Hiser L, Herrington B, Lobert S. Effect of noscapine and vincristine combination on demyelination and cell proliferation in vitro. *Leuk Lymphoma*. 2008; 49:1603–9. [PubMed: 18766974]
20. Bunn PA Jr. Treatment of advanced non-small-cell lung cancer with two-drug combinations. *J Clin Oncol*. 2002; 20:3565–7. [PubMed: 12202651]
21. Hasturk S, Hatabay N, Ece F, Karatasli M, Hanta I. Gemcitabine, Vinorelbine, and cisplatin in the treatment of advanced nonsmall cell lung cancer. *Am J Clin Oncol*. 2009; 32:280–5. [PubMed: 19433960]
22. Bigioni M, Benzo A, Irrissuto C, Lopez G, Curatella B, Maggi CA, et al. Anti-tumour effect of combination treatment with Sabarubicin (MEN 10755) and cis-platin (DDP) in human lung tumour xenograft. *Cancer Chemother Pharmacol*. 2008; 62:621–9. [PubMed: 18038274]
23. Soriano AF, Helfrich B, Chan DC, Heasley LE, Bunn PA Jr, Chou TC. Synergistic effects of new chemopreventive agents and conventional cytotoxic agents against human lung cancer cell lines. *Cancer Res*. 1999; 59:6178–84. [PubMed: 10626810]
24. Jiang QQ, Fan LY, Yang GL, Guo WH, Hou WL, Chen LJ, et al. Improved therapeutic effectiveness by combining liposomal honokiol with cisplatin in lung cancer model. *BMC Cancer*. 2008; 8:242. [PubMed: 18706101]
25. Nagano T, Yasunaga M, Goto K, Kenmotsu H, Koga Y, Kuroda J, et al. Antitumor activity of NK012 combined with cisplatin against small cell lung cancer and intestinal mucosal changes in tumor-bearing mouse after treatment. *Clin Cancer Res*. 2009; 15:4348–55. [PubMed: 19509138]

26. Wu XX, Kakehi Y. Enhancement of lextatumumab-induced apoptosis in human solid cancer cells by Cisplatin in caspase-dependent manner. *Clin Cancer Res.* 2009; 15:2039–47. [PubMed: 19276256]
27. Vasvari GP, Dyckhoff G, Kashfi F, Lemke B, Lohr J, Helmke BM, et al. Combination of thalidomide and cisplatin in an head and neck squamous cell carcinomas model results in an enhanced antiangiogenic activity in vitro and in vivo. *Int J Cancer.* 2007; 121:1697–704. [PubMed: 17557286]
28. Liu X, Chan SY, Ho PC. Comparison of the in vitro and in vivo effects of retinoids either alone or in combination with cisplatin and 5-fluorouracil on tumor development and metastasis of melanoma. *Cancer Chemother Pharmacol.* 2008; 63:167–74. [PubMed: 18465132]
29. Menendez JA, del Mar Barbacid M, Montero S, Sevilla E, Escrich E, Solanas M, et al. Effects of gamma-linolenic acid and oleic acid on paclitaxel cytotoxicity in human breast cancer cells. *Eur J Cancer.* 2001; 37:402–13. [PubMed: 11239764]
30. Ichite N, Chougule MB, Jackson T, Fulzele SV, Safe S, Singh M. Enhancement of docetaxel anticancer activity by a novel diindolylmethane compound in human non-small cell lung cancer. *Clin Cancer Res.* 2009; 15:543–52. [PubMed: 19147759]
31. Hohla F, Schally AV, Kanashiro CA, Buchholz S, Baker B, Kannadka C, et al. Growth inhibition of non-small-cell lung carcinoma by BN/GRP antagonist is linked with suppression of K-Ras, COX-2, and pAkt. *Proc Natl Acad Sci USA.* 2007; 104:18671–6. [PubMed: 18003891]
32. Aneja R, Ghaleb AM, Zhou J, Yang VW, Joshi HC. p53 and p21 determine the sensitivity of noscapine-induced apoptosis in colon cancer cells. *Cancer Res.* 2007; 67:3862–70. [PubMed: 17440101]
33. Antonsson B. Bax and other pro-apoptotic Bcl-2 family “killer-proteins” and their victim the mitochondrion. *Cell Tissue Res.* 2001; 306:347–61. [PubMed: 11735035]
34. Kawasaki H, Toyoda M, Shinohara H, Okuda J, Watanabe I, Yamamoto T, et al. Expression of survivin correlates with apoptosis, proliferation, and angiogenesis during human colorectal tumorigenesis. *Cancer.* 2001; 91:2026–32. [PubMed: 11391581]
35. Sung B, Ahn KS, Aggarwal BB. Noscapine, a benzyloquinoline alkaloid, sensitizes leukemic cells to chemotherapeutic agents and cytokines by modulating the NF-kappaB signaling pathway. *Cancer Res.* 2010; 70(8):3259–68. [PubMed: 20354190]
36. Karlsson MO, Dahlstrom B, Eckernas SA, Johansson M, Alm AT. Pharmacokinetics of oral noscapine. *Eur J Clin Pharmacol.* 1990; 39:275–9. [PubMed: 2257866]
37. Aneja R, Dhiman N, Idnani J, Awasthi A, Arora SK, Chandra R, et al. Pre-clinical pharmacokinetics and bioavailability of noscapine, a tubulin-binding anticancer agent. *Cancer Chemother Pharmacol.* 2007; 60:831–9. [PubMed: 17285314]
38. Dahlstrom B, Mellstrand T, Lofdahl CG, Johansson M. Pharmacokinetic properties of noscapine. *Eur J Clin Pharmacol.* 1982; 22M:535–9. [PubMed: 7128665]
39. Myung J, Kim KB, Crews CM. The ubiquitin–proteasome pathway and proteasome inhibitors. *Med Res Rev.* 2001; 21:245–73. [PubMed: 11410931]
40. Mousavi-Shafaei P, Ziaee AA, Zangemeister-Wittke U. Increased cytotoxicity of cisplatin in SK-MEL 28 melanoma cells upon down-regulation of melanoma inhibitor of apoptosis protein. *Iran Biomed J.* 2009; 13:27–34. [PubMed: 19252675]
41. Mabuchi S, Altomare DA, Cheung M, Zhang L, Poulidakos PI, Hensley HH, et al. RAD001 inhibits human ovarian cancer cell proliferation, enhances cisplatin-induced apoptosis, and prolongs survival in an ovarian cancer model. *Clin Cancer Res.* 2007; 13:4261–70. [PubMed: 17634556]

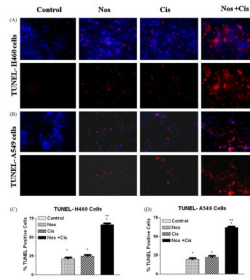


Fig. 1. Micrographs of cells stained with TUNEL after 72 h (A) with Cis 0.8 μ M, Nos 30 μ M, and, Cis 0.8 μ M + Nos 30 μ M in H460 cells; (B) Cis 2.5 μ M, Nos 40 μ M, and, Cis 2.5 μ M + Nos 40 μ M in A549 cells; quantitation of apoptotic H460 (C) and A549 (D) cells from TUNEL assay. The apoptotic cells were detected using ApoTag Red *In Situ* Apoptosis detection kit[®]. DNA fragmentation is indicated by Rhodamine positive staining (red). Control cells were untreated. Micron bar = 20 μ m. Cells were quantitated by counting 100 cells from 6 random microscopic fields. Data are expressed as mean + SD ($N = 6$). One-way ANOVA followed by post-Tukey test was used for statistical analysis to compare control and treated groups. * $P < 0.01$; all treatments significantly different from control and ** $P < 0.01$; significantly different from Nos and Cis single treatments. (For interpretation of the references to color in this figure legend, the reader is referred to the web version of the article.)

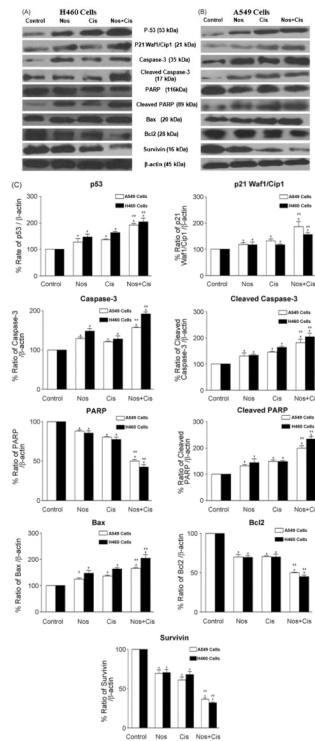


Fig. 2. Expression of p53, p21, caspase 3, cleaved caspase 3, PARP, cleaved PARP, Bax, Bcl₂, survivin in H460 (A) and A549 (B) tumor cell lysates by western blotting and (C) quantitation of apoptotic protein expression. H460 cells were treated with Cis (0.8 μ M), Nos (30 μ M), and Cis (0.8 μ M) + Nos (30 μ M) and A549 cells were treated with Cis (2.5 μ M), Nos (40 μ M), and Cis (2.58 μ M) + Nos (40 μ M) for 72 h and whole-cell lysates were analyzed by western blotting for protein expression. Protein expression levels (relative to β -actin) were determined. Mean \pm SE for three replicate determinations. One-way ANOVA followed by post-Tukey test was used for statistical analysis. $P < 0.01$ (*significantly different from untreated controls; **significantly different from Nos and Cis single treatments).

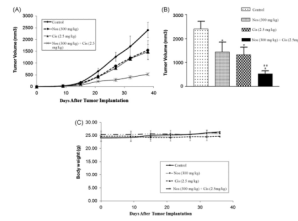


Fig. 3.

Effects of Nos and Cis on human H460 lung tumor xenograft model (A) progression profile of tumor growth kinetics (B) tumor volume measurements on day 38 after tumor implantation (tumor volumes, mm³ ± SEM), and (C) measurement of body weight. Female nude mice with xenograft lung tumors received various treatments for 38 days starting on day 7 after tumor implantation. The mice were treated with Cis 2.5 mg/kg i.v. (q4d × 3 schedule), Nos 300 mg/kg/day, and Cis + Nos. Control group received vehicle only. Statistical significance of the difference in lung weights of treatment groups compared with control. $P < 0.01$ (*significantly different from untreated controls; **significantly different from Nos and Cis single treatments). Data presented are means and SE ($n = 8$). This experiment was repeated twice.

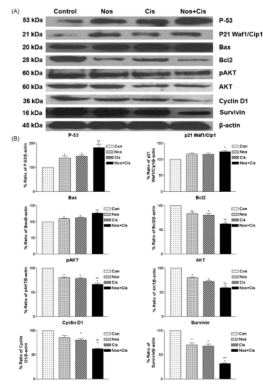


Fig. 4.

Expression of p53, p21, pAkt, survivin, cyclin D1, Bax, and Bcl₂ proteins in tumor lysates by western blotting (A) and (B) quantitation of apoptotic protein expression. Lane 1, untreated control tumors; lane 2, oral Nos 300 mg/kg; lane 3, Cis 2.5 mg/kg i.v. (q4d × 3 schedule); lane 4; Cis + Nos. β-Actin protein acts as a loading control. Similar results were observed in triplicate experiments. Protein expression levels (relative to β-actin) were determined. Mean ± SE for three replicate determinations. One-way ANOVA followed by post-Tukey test was used for statistical analysis. $P < 0.01$ (*significantly different from untreated controls; **significantly different from Nos and Cis single treatments).

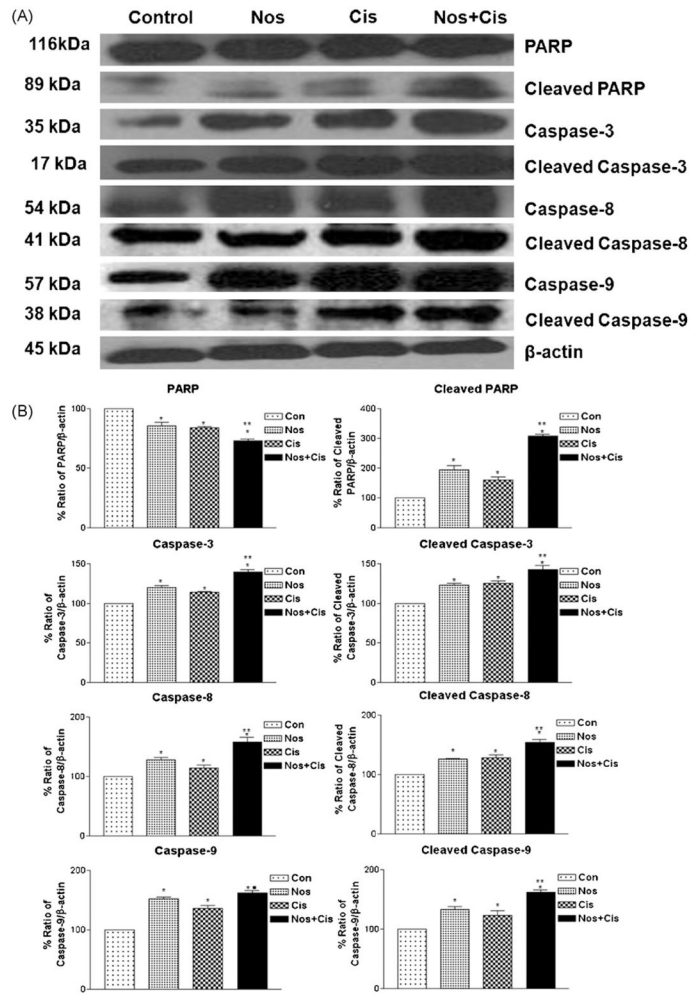


Fig. 5. Expression of apoptotic proteins in tumors (A) and (B) quantitation of apoptotic protein expression. Whole-cell lysates from control-untreated and treated tumors were analyzed by western blotting for PARP, cleaved PARP, caspase 3, 8 and 9 protein expressions. Lane 1, untreated control tumors; lane 2, oral Nos 300 mg/kg; lane 3, Cis 2.5 mg/kg i.v. (q4d \times 3 schedule); lane 4; Cis + Nos. β -Actin protein acts as a loading control. Similar results were observed in replicate experiments. Protein expression levels (relative to β -actin) were determined. Mean \pm SE for three replicate determinations. One-way ANOVA followed by post-Tukey test was used for statistical analysis. $P < 0.01$ (*significantly different from untreated controls; **significantly different from Nos and Cis single treatments; ■ significantly different from Cis single treatment).

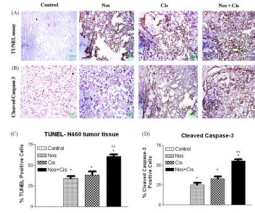


Fig. 6. Immunohistochemical staining of xenograft H460 lung tumor tissues for induction of apoptosis using TUNEL assay (A); for expression of cleaved caspase 3 (B); quantitation of apoptotic cells from TUNEL staining (C); and quantitation of cleaved caspase 3-positive cells apoptotic cells (D). Tumor tissues were dissected from mice on day 38, fixed in 10% formalin, paraffin embedded and sectioned. Sections were stained using the DeadEnd colorimetric kit and cleaved caspase 3 (Asp 175) IHC kit for TUNEL assay and cleaved caspase 3 expression as described in Section 2 respectively. The apoptotic tumor cells are stained brown. Percentages of TUNEL-positive and cleaved caspase 3-positive cells were quantitated by counting 100 cells from 6 random microscopic fields. Data are expressed as mean + SD ($N = 6$). One-way ANOVA followed by post-Tukey test was used for statistical analysis to compare control and treated groups. $P < 0.01$ (*significantly different from untreated controls; **significantly different from Nos and Cis single treatments). Original magnification 40 \times (micron bar = 50 μm).

Table 1

Combination index (CI) values of the interaction between Cis with Nos (μM) against human lung cancer cells.

H460		A549	
Drug combinations	CI at IC₅₀	Interpretation	Drug combinations
Cis + Nos 10	0.31 ± 0.05	Strong synergism	Cis + Nos 30
Cis + Nos 15	0.43 ± 0.03	Strong synergism	Cis + Nos 40
Cis + Nos 20	0.57 ± 0.08	Synergism	Cis + Nos 50
			CI at IC₅₀
			0.37 ± 0.03
			0.49 ± 0.07
			0.57 ± 0.04
			Interpretation
			Strong synergism
			Synergism
			Synergism

The human lung cancer cell lines A549 (adenocarcinoma) and large-cell carcinoma type H460 (large-cell carcinoma) were obtained from American Type Culture Collection (Rockville, MD). Different concentrations of Nos were employed to study the effect on IC₅₀ of Cis. Variable ratios of drug concentrations and mutually non-exclusive equations were used to determine the CI. The CI values represent mean of four experiments. CI > 1.3: antagonism; CI 1.1–1.3: moderate antagonism; CI 0.9–1.1: additive effect; CI 0.8–0.9: slight synergism; CI 0.6–0.8: moderate synergism; CI 0.4–0.6: synergism; CI 0.2–0.4: strong synergism.